

San Jose State University

SJSU ScholarWorks

Faculty Publications, Chemistry

Chemistry

1-1-2002

Familial ALS-Associated Mutations Decrease the Thermal Stability of Distinctly Metallated Species of Human Copper/Zinc Superoxide Dismutase

Daryl K. Eggers

San Jose State University, daryl.eggars@sjsu.edu

J. A. Rodriguez

University of California, Los Angeles

J. S. Valentine

University of California, Los Angeles

J. A. Roe

Loyola Marymount University

A. Tiwari

University of Massachusetts Medical School

See next page for additional authors

Follow this and additional works at: https://scholarworks.sjsu.edu/chem_pub



Part of the [Biochemistry Commons](#), and the [Other Chemistry Commons](#)

Recommended Citation

Daryl K. Eggers, J. A. Rodriguez, J. S. Valentine, J. A. Roe, A. Tiwari, R. H. Brown, and L. J. Hayward. "Familial ALS-Associated Mutations Decrease the Thermal Stability of Distinctly Metallated Species of Human Copper/Zinc Superoxide Dismutase" *The Journal of Biological Chemistry* (2002): 15932-15937. <https://doi.org/10.1074/jbc.M112088200>

This Article is brought to you for free and open access by the Chemistry at SJSU ScholarWorks. It has been accepted for inclusion in Faculty Publications, Chemistry by an authorized administrator of SJSU ScholarWorks. For more information, please contact scholarworks@sjsu.edu.

Authors

Daryl K. Eggers, J. A. Rodriguez, J. S. Valentine, J. A. Roe, A. Tiwari, R. H. Brown, and L. J. Hayward

Familial Amyotrophic Lateral Sclerosis-associated Mutations Decrease the Thermal Stability of Distinctly Metallated Species of Human Copper/Zinc Superoxide Dismutase*

Received for publication, December 18, 2001, and in revised form, February 12, 2002
Published, JBC Papers in Press, February 19, 2002, DOI 10.1074/jbc.M112088200

Jorge A. Rodriguez, Joan S. Valentine, Daryl K. Eggers, James A. Roe‡, Ashutosh Tiwari§, Robert H. Brown, Jr.¶, and Lawrence J. Hayward§||

From the Department of Chemistry and Biochemistry, UCLA, Los Angeles, California 90095-1569, the ‡Department of Chemistry and Biochemistry, Loyola Marymount University, Los Angeles, California 90045-8225, the ¶Department of Neurology, Massachusetts General Hospital, Charlestown, Massachusetts 02129, and the §Department of Neurology, University of Massachusetts Medical School, Worcester, Massachusetts 01655

We report the thermal stability of wild type (WT) and 14 different variants of human copper/zinc superoxide dismutase (SOD1) associated with familial amyotrophic lateral sclerosis (FALS). Multiple endothermic unfolding transitions were observed by differential scanning calorimetry for partially metallated SOD1 enzymes isolated from a baculovirus system. We correlated the metal ion contents of SOD1 variants with the occurrence of distinct melting transitions. Altered thermal stability upon reduction of copper with dithionite identified transitions resulting from the unfolding of copper-containing SOD1 species. We demonstrated that copper or zinc binding to a subset of “WT-like” FALS mutants (A4V, L38V, G41S, G72S, D76Y, D90A, G93A, and E133A) conferred a similar degree of incremental stabilization as did metal ion binding to WT SOD1. However, these mutants were all destabilized by ~1–6 °C compared with the corresponding WT SOD1 species. Most of the “metal binding region” FALS mutants (H46R, G85R, D124V, D125H, and S134N) exhibited transitions that probably resulted from unfolding of metal-free species at ~4–12 °C below the observed melting of the least stable WT species. We conclude that decreased conformational stability shared by all of these mutant SOD1s may contribute to SOD1 toxicity in FALS.

Copper/zinc superoxide dismutase (SOD1)¹ catalyzes the disproportionation of two molecules of superoxide anion (O₂⁻) into O₂ and H₂O₂ (1, 2) in all eukaryotic cells. Many specific, highly conserved structural interactions confer upon SOD1 a remarkable thermal stability (3–6) and resistance to chemical denaturation (7–9).

* This work was supported by grants from the ALS Association (to L. J. H. and J. S. V.); National Institutes of Health Grants GM28222 (to J. S. V.) and PO1NS31248 and PO1NS37912 (to R. H. B.); and the Cecil B. Day Neuromuscular Research Laboratory (to R. H. B.). DSC experiments were performed in the UCLA-Department of Energy Biochemistry Instrumentation Facility under the guidance of M. Phillips. The costs of publication of this article were defrayed in part by the payment of page charges. This article must therefore be hereby marked “advertisement” in accordance with 18 U.S.C. Section 1734 solely to indicate this fact.

|| To whom correspondence should be addressed: Dept. of Neurology, University of Massachusetts Medical School, 55 Lake Ave. N., Worcester, MA 01655. Tel.: 508-334-4007; Fax: 508-334-2756; E-mail: Lawrence.Hayward@umassmed.edu.

¹ The abbreviations used are: SOD1, copper/zinc superoxide dismutase; WT, wild type; ALS, amyotrophic lateral sclerosis; FALS, familial ALS; DSC, differential scanning calorimetry; O₂⁻, superoxide.

Each subunit of homodimeric SOD1 is built upon a flattened β-barrel motif with additional loop regions that contribute to metal ion binding and formation of the active site (10). One catalytic copper ion and one buried zinc ion per subunit are bound at the active site on the external surface of the β-barrel. Occupancy of the metal ion binding sites confers greater thermal stabilization to the bovine SOD1 apoenzyme (3, 4). The copper and zinc ions are linked directly via the imidazole side chain of the shared His-63 residue² and indirectly via extended interactions between their respective ligands. SOD1 dimerization is stabilized by optimized hydrophobic interactions at the contact interface between complementary patches on each subunit (10–12). A conserved intrasubunit disulfide bond involving Cys-57 also stabilizes the enzyme by anchoring a loop that forms part of the dimer interface to the β-barrel at Cys-146.

A subset of SOD1 mutations in familial amyotrophic lateral sclerosis (FALS) have been proposed to destabilize the β-barrel or disrupt dimerization of SOD1 monomers (13, 14). A crystal structure obtained for the G37R SOD1 mutant shows minimal perturbation of the averaged backbone conformation but exhibits unusually high atomic displacement parameters, suggestive of increased molecular flexibility in some regions of the molecule (15). Consistent with this, some mutant SOD1s exhibit accelerated turnover *in vivo* (16, 17) or increased susceptibility to proteolytic digestion (17) compared with the wild type (WT) enzyme. However, a quantitative analysis of FALS mutant SOD1 structural stability and its relation to metal occupancy has not been reported.

In the present study, we investigated the effects of 14 ALS-associated mutations on the thermodynamic stability of biologically metallated human SOD1s. Using differential scanning calorimetry (DSC), we measured the melting temperatures (*T_m*) of WT SOD1 and mutant variants hypothesized to perturb the active site region, the dimer interface, one pole of the β-barrel, and associated loops. We distinguished the melting properties of partially metallated SOD1 species and showed that mutant SOD1 proteins were destabilized relative to the corresponding WT species.

EXPERIMENTAL PROCEDURES

SOD1 Sample Preparation—Recombinant human WT and mutant SOD1 enzymes (A4V, L38V, G41S, H46R, H48Q, G72S, D76Y, G85R, D90A, G93A, D124V, D125H, E133A, and S134N) were expressed in a baculovirus/Sf21 insect cell system and purified as previously described (18). Protein concentrations were estimated using a dimeric molar

² SOD1 residues are numbered according to those in the human enzyme.

extinction coefficient at 280 nm of 10,800 $M^{-1}cm^{-1}$ (19) or 13,800 $M^{-1}cm^{-1}$ for D76Y SOD1 (20). The copper and zinc contents of these biologically metallated proteins were previously determined by inductively coupled plasma mass spectrometry (18). SOD1 protein concentrations were adjusted to 2 mg/ml for all samples in a reference buffer containing 50 mM KCl and 100 mM potassium phosphate, pH 7.2. Cu(II) was reduced to Cu(I) in some samples immediately before calorimetric analysis by the addition of a small excess of dithionite (5).

Differential Scanning Calorimetry—The thermal stability of WT SOD1 and FALS-associated mutant SOD1s was measured using a Nano II differential scanning calorimeter (Calorimetry Sciences Corp.). The calorimeter was equipped with two U-shaped cells, a reference cell and a sample cell, each with a capacity of 326.8 μ l. In all DSC experiments, the sample cell was filled with a protein solution in the same buffer used to fill the reference cell. All buffers and protein solutions were degassed for 15 min using a vacuum generated by a water aspirator. A buffer *versus* buffer base line was measured prior to the calorimetric analysis of protein samples. All samples were run in duplicate through a temperature range of 25–100 °C at a rate of 1 °C/min under 3 atm of pressure.

Analysis of Calorimetric Data—CpCalc software (Calorimetry Sciences Corp.) was used to determine molar heat capacity values, and Origin software (Microcal) was used to fit the data to a non-two-state thermal transition model (21), which has been used previously for DSC studies of SOD1 (5). Base line curves were derived by connecting the pre- and post-transition base lines. Each T_m value was determined within an error of ± 0.5 °C, unless otherwise specified, after deconvolution of the DSC profiles into individual components. Summation of the deconvoluted components agreed well with the observed DSC traces. It was not possible to determine accurate enthalpy values for many of the endotherms at higher temperatures due to the irreversible melting behavior of human WT and FALS-associated SOD1s. However, sharp exothermic transitions typical of aggregation mainly occurred after a given endothermic unfolding peak had already formed in the DSC profiles. Therefore, T_m values were less affected by aggregation and were used to compare relative thermal stabilities of the enzymes.

RESULTS

Melting of WT SOD1 Produced Three Endotherms—The heat-induced unfolding of a partially metallated sample of human WT SOD1 produced a DSC profile consisting of multiple overlapping endothermic transitions (Fig. 1A). Deconvolution of the DSC trace using a non-two-state transition model yielded three endotherms, consistent with the unfolding of differentially metallated SOD1 species (5). T_m values obtained for the three transitions of this WT SOD1 sample were 60.8, 75.7, and 83.7 °C and were denoted as T_{m1} , T_{m2} , and T_{m3} , respectively (Fig. 1A). The occurrence of multiple endotherms was not surprising, because these biologically metallated SOD1 enzymes that were overexpressed in insect cells exhibited incomplete metal occupancy (18).

DSC measurements reflect the sum of any endothermic (*e.g.* unfolding) or exothermic (*e.g.* aggregation) processes during slow heating of the sample. As has been noted in previous DSC studies, SOD1 undergoes irreversible unfolding upon heating to high temperatures (5, 22). Because the apparent molar enthalpy for a given transition depends on the area under the endotherm, aggregation during the DSC scan may contribute to underestimation of the true enthalpy of SOD1 denaturation. However, the T_m values of the DSC transitions, which were highly reproducible from run to run, served as a useful estimate of relative thermostability. The deconvolution model for obtaining the T_m values was validated by the close alignment of the experimental and calculated traces (Fig. 1B).

Metal Ion Binding Favored Increased Stability of Mutant SOD1s—To observe the influence of metal binding upon SOD1 stability, we performed DSC upon two differentially metallated samples for each of the WT, H46R, D76Y, G85R, and E133 Δ SOD1 proteins. Occupancy of the copper and zinc binding sites for these samples (Table I) was influenced either by metal ion

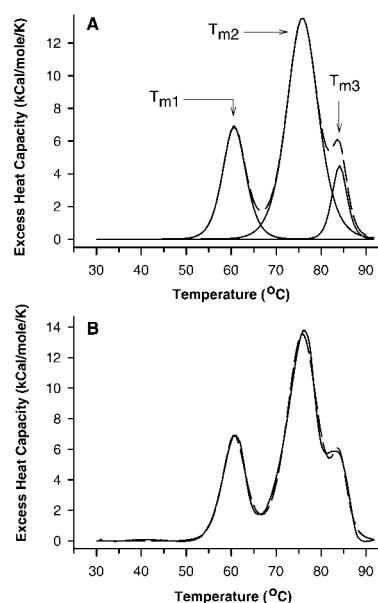


FIG. 1. Three endotherms were observed upon thermal unfolding of partially metallated human WT SOD1. A, overlay of the best fit curve (*dashed line*) and the individual transitions (*solid lines*) obtained from deconvolution of the DSC profile for the WT-A SOD1 sample, which contained 0.31 eq of copper and 1.50 eq of zinc ions per dimer (Table I). The midpoints of the three transitions were denoted T_{m1} , T_{m2} , and T_{m3} . B, the best fit curve (*dashed line*) superimposed with the actual DSC trace of WT-A SOD1 (*solid line*). DSC conditions for all samples were as follows: 2 mg/ml SOD1 protein in 50 mM KCl, 100 mM potassium phosphate buffer, pH 7.2; scan rate = 1 °C/min; pressure = 3 atm.

supplementation to the medium during protein expression (for the WT, H46R, or G85R samples) or by fractionation during ion exchange chromatography (for the D76Y and E133 Δ samples) (18).

DSC scans for E133 Δ -1 and E133 Δ -2 samples in Fig. 2A each exhibited two distinct endotherms, centered near 55 and 71 °C, and an overlapping transition near 76 °C that appeared as a smaller shoulder. An exothermic transition above 80 °C most likely reflected aggregation of the sample. E133 Δ -1, which contained more metal ions than did E133 Δ -2, yielded a smaller endotherm at 55.9 °C and larger endotherms relative to E133 Δ -2 at 71.9 and 76.8 °C. This suggested that the species unfolding during the two more stable transitions had greater metal occupancy than did the species producing the least stable endotherm. A similar effect of metal ion content on endotherm magnitudes was observed for the differentially metallated fractions of D76Y SOD1 (not shown).

Substitution of a copper ligand with arginine in H46R SOD1 abolished Cu(II) ion binding to the catalytic site and also altered the zinc binding site (23). We compared preparations of H46R purified from cells grown in medium supplemented with either a 50 μ M (H46R-A) or 300 μ M (H46R-B) concentration of copper and zinc ions. H46R-B contained a small but significant amount of zinc that was not present in H46R-A (Table I). DSC scans of H46R-A exhibited a single transition near 56 °C that reflected unfolding of the metal-free protein (Fig. 2B). For H46R-B, binding of 0.07 equivalents of zinc per dimer correlated with a decrease in the magnitude of the main transition and the appearance of a new endotherm near 72 °C. These data suggested that zinc binding increased the T_m for H46R SOD1 by 16 °C. This stabilization paralleled the difference between T_{m2} and T_{m1} observed for both WT and E133 Δ human SOD1s (Table I) and was also consistent with a previous study showing that zinc binding to bovine SOD1 apoenzyme increases its T_m by 13 °C (5).

TABLE I
Summary of WT and mutant SOD1 thermal stabilities

T_{m1} , T_{m2} , T_{m3} , and T_{m4} represent the melting temperatures of distinct WT or mutant SOD1 species in our as-isolated protein samples. Melting temperatures were averaged from two independent DSC profiles after deconvolution of the corresponding endotherms. T_m values marked with an asterisk were derived from deconvolution of a single endotherm if the duplicate scan exhibited excessive sample aggregation.

SOD1 protein ^a	Equivalents/dimer		T_{m1}	T_{m2}	T_{m3}	T_{m4}	$T_{m2} - T_{m1}$	$T_{m3} - T_{m1}$
	Copper	Zinc						
WT-A	0.31	1.50	60.8	75.7	83.7		15.0	22.9
WT-B	0.57	1.74	60.4	76.7	83.1		16.3	22.7
WT-like mutants								
A4V	0.21	1.69	54.0	67.9	76.4		13.9	22.4
L38V	0.34	0.87	56.5	72.5	80.2		16.0	23.7
G41S	0.52	1.35	54.5	70.6	78.5	89.8	16.1	24.1
G72S	0.74	0.78	54.9*	69.0	75.5	88.9	14.2	20.6
D76Y-1	0.58	1.27	55.6	71.2	78.7*	90.2*	15.7	23.1
D76Y-2	0.36	0.82	54.5	69.9	78.3*		15.4	23.8
D90A	0.34	1.77	59.8	75.5	82.9		15.7	23.1
G93A	0.45	1.46	58.3	74.1	82.8	91.6	15.8	24.4
E133Δ-1	0.31	1.26	55.9	71.9	76.8		16.0	20.9
E133Δ-2	0.16	0.84	55.1	70.7	75.5		15.6	20.5
Metal-binding region mutants ^b								
H46R-A	0	0.01	56.5					
H46R-B	0.02	0.07	55.3	71.7				
H48Q	0.63	1.08	60.9	80.2	87.2			
G85R-A	ND ^c	ND	48.8	57.7	71.8	81.5		
G85R-B	0	0.01	49.0	59.6				
D124V	0.01	0.03	54.1	57.8				
D125H	0.09	0.36	54.0	82.8				
S134N	0.15	0.33	54.3	68.4				

^a Protein names indexed by letters (A or B) denote samples purified from Sf21 cells grown in medium supplemented with either 50 μM (A) or 300 μM (B) cupric chloride and zinc chloride. Protein names indexed by numbers (1 or 2) denote two separate chromatographic fractions obtained from the same cell suspension. E133Δ denotes a deletion of the Glu-133 residue alone (29) rather than a truncation of the protein.

^b The transitions at T_{m1} , T_{m2} , T_{m3} , and T_{m4} for the metal-binding region mutants, which typically contained less copper or zinc than did the WT-like mutants, could not be definitively assigned to corresponding transitions of the WT-like proteins. Therefore, the differences $T_{m2} - T_{m1}$ and $T_{m3} - T_{m1}$ are not indicated for metal-binding region mutants.

^c ND, not determined.

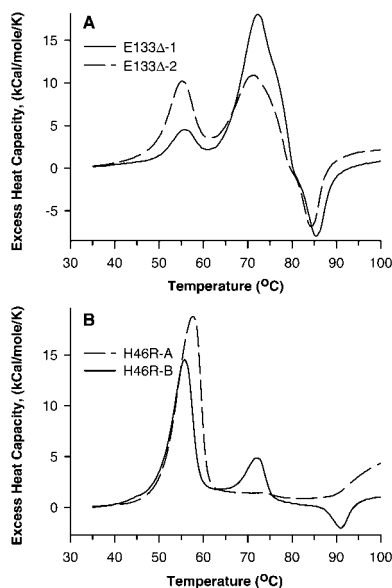


FIG. 2. **Metal ion binding stabilized SOD1 mutants.** A, DSC profiles from two differentially metallated samples of the single-residue deletion mutant E133Δ. Fraction E133Δ-1 contained more copper and zinc than did fraction E133Δ-2 (Table I). B, DSC profiles from two separate preparations of H46R SOD1 from cells grown in medium supplemented with either a 50 μM (H46R-A) or 300 μM (H46R-B) concentration of copper and zinc ions. Metal contents after purification are listed in Table I.

Copper Reduction Identified the Unfolding of Copper-containing Species—Reduction of copper in the fully metallated bovine SOD1 enzyme increases its thermal stability by 4 °C compared with the oxidized form under similar scan conditions (5). To discern which endotherm(s) represented the unfolding of

a copper-containing species, we reduced Cu(II) to Cu(I) in samples of WT and A4V SOD1 proteins by incubation with dithionite. Fig. 3A shows that WT SOD1 reduced by dithionite exhibited an increase in T_{m3} from 83.3 to 86.1 °C, while T_{m1} and T_{m2} remained unchanged. A similar effect was observed in the reduced form of the A4V mutant, with a shift in T_{m3} from 76.6 to 80.5 °C (Fig. 3B). The increase in T_{m3} may be related to relaxation of strain in the protein upon rearrangement of the ligand geometry to that preferred by Cu(I). These results implicated the endotherm at T_{m3} as the unfolding transition of a species that contained copper.

A Subset of FALS Mutants Exhibited Corresponding yet Destabilized Transitions Relative to WT SOD1—We previously identified eight mutants (A4V, L38V, G41S, G72S, D76Y, D90A, G93A, and E133Δ) that shared “WT-like” copper coordination and full activity of bound copper (18). In the present experiments, we observed that the DSC profiles for these mutants each contained multiple endotherms that probably reflected unfolding of distinctly metallated species, as was seen for the WT protein. These transitions were labeled numerically from lowest to highest T_m value observed for each mutant (Table I; T_{m1} , T_{m2} , T_{m3} , and T_{m4}). The lowest melting transition for each WT-like mutant was destabilized by an average of 4.7 ± 1.8 °C (range 0.8–6.6 °C, Table I) compared with the corresponding transition for the WT protein.

The three major melting transitions observed for the A4V and L38V mutant species are compared with those for WT SOD1 in Fig. 4. While the extent of destabilization varied among different mutants, all three transitions for a given mutant exhibited a comparable instability with respect to the corresponding WT SOD1 transitions. The difference in temperature between T_{m1} and T_{m2} remained nearly constant (14–16 °C) for all of these WT-like mutants (Table I). Similarly, the T_m associated with the copper-containing species, T_{m3} , was

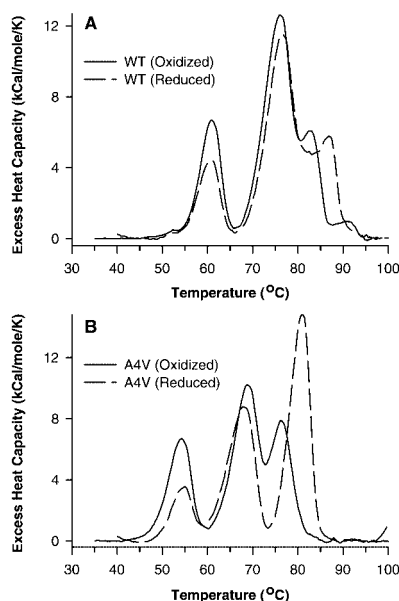


FIG. 3. Unfolding of oxidized and reduced copper-containing SOD1 species. Reduction of the copper ion in WT (A) or A4V (B) SOD1s by dithionite did not affect the T_m of the two least stable species but increased the T_m of the most stable species (T_{m3}). DSC traces are shown for untreated SOD1 samples (solid lines) and proteins incubated with dithionite immediately before DSC (dashed lines).

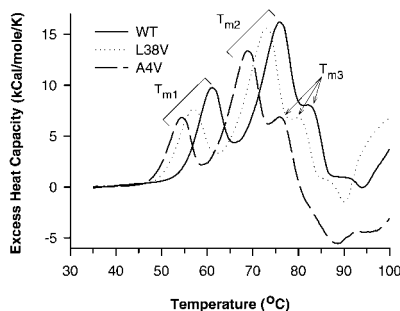


FIG. 4. Partially metallated SOD1 FALS mutants were destabilized compared with WT SOD1. The DSC profiles of as isolated WT (solid line), L38V (dotted line), and A4V (dashed line) SOD1 proteins were each characterized by three transitions denoted T_{m1} , T_{m2} , and T_{m3} . While different mutants exhibited variation in the degree of destabilization, all three transitions for a given mutant protein were destabilized to the same extent when compared with the corresponding transitions for WT SOD1.

21–24 °C higher than T_{m1} for each WT-like mutant (Table I). This suggested that binding of metal ions to either the WT or WT-like mutant enzymes afforded a similar incremental gain in stability.

The four WT-like mutants G41S, G72S, D76Y, and G93A exhibited an additional endotherm centered near 90 °C (Table I), as shown in the profiles of G41S and G93A SOD1s (Fig. 5). The melting temperature associated with this endotherm (T_{m4}) was consistently 33–35 °C higher than T_{m1} . Under the same DSC conditions, we observed a major melting transition at 93 °C for fully metallated human WT SOD1 isolated from erythrocytes (not shown). This suggested that T_{m4} corresponded to unfolding of a subpopulation of fully metallated dimers.

DSC Profiles of Severely Metal-deficient SOD1s—Five “metal-binding region” SOD1 mutants (H46R, G85R, D124V, D125H, and S134N) were severely metal-deficient (18), indicating that the metal-free apoprotein was the main constituent of these samples (Table I). The mutants G85R, D124V, and D125H exhibited unique DSC profiles (Fig. 6) and transitions

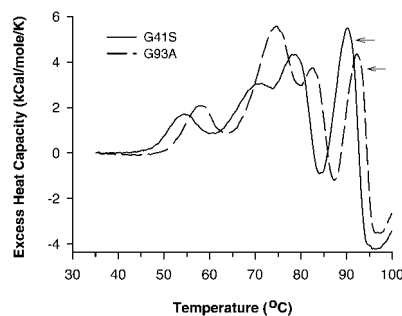


FIG. 5. DSC profiles of G41S and G93A revealed a fourth melting transition. The arrows point to the new transition, denoted T_{m4} in Table I. The melting temperature of this transition was similar to that measured for the fully metallated form of human and bovine SOD1.

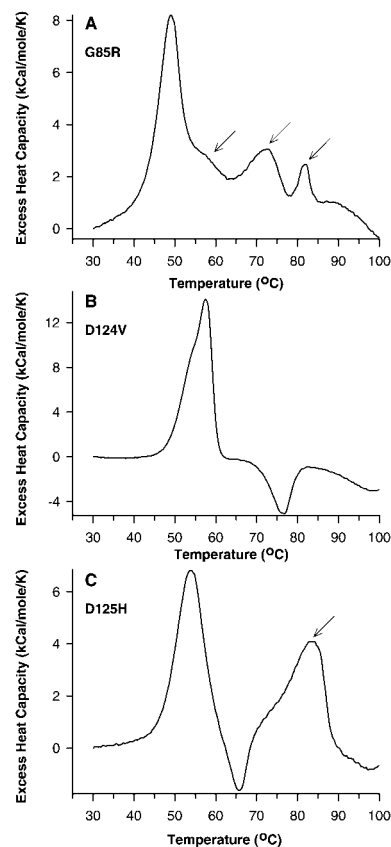


FIG. 6. Thermal stabilities of metal-binding region mutants. The DSC profiles of mutants G85R (A), D124V (B), and D125H (C) differed significantly from the WT-like mutants. The first transition for each mutant SOD1 protein most likely corresponded to unfolding of the metal-free protein. The arrows point to additional endotherms of uncertain origin.

that could not be directly correlated with those of the “WT-like” mutants, which were likely to contain much less apoprotein according to the metal content analysis.

The G85R mutant exhibited a main transition centered at 49 °C (Fig. 6A) and was the most destabilized species that we observed. Moreover, G85R SOD1 began to unfold at the near physiological temperature of 42 °C. This major transition most likely arose from melting of the G85R apoprotein, while minor transitions seen at 58, 72, and 82 °C may have represented unfolding of partially metallated species.

The DSC profile of D124V was composed of a shoulder at 54.1 °C and a main transition at 57.8 °C (Fig. 6B). Because metals were almost undetectable in the D124V sample (Table I), this result suggested that the endotherms near 56 °C arose from melting of a metal-free protein. The precise species that

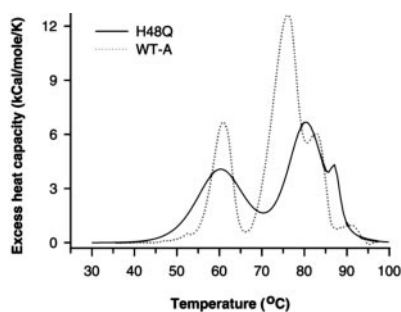


FIG. 7. **Thermal stability of H48Q SOD1.** DSC profiles of H48Q (solid line) and WT-A (dotted line) SOD1 samples. The least stable form of H48Q began to unfold $\sim 5^\circ\text{C}$ below that of WT SOD1.

produced these two overlapping transitions and possible cooperative unfolding interactions remain to be clarified. The exotherm near 76°C most likely arose from aggregation or precipitation of unfolded proteins.

The DSC profile of the D125H mutant exhibited a major endotherm at 54.0°C that evolved into a prominent exotherm, probably related to aggregation or precipitation, as the temperature approached 66°C (Fig. 6C). Given the low metal content of D125H SOD1, it is likely that the transition at 54.0°C arose from melting of an apoprotein and that the transition at 82.8°C was produced by unfolding of either a metal-containing species or an unusually stable, nonnative form of the enzyme.

H48Q SOD1 Exhibited Decreased Cooperativity of Unfolding Compared with WT SOD1—The H48Q mutant contained substantial amounts of copper and zinc ions (Table I) when compared with other metal binding region mutants yet contained less zinc than the WT samples (18). The DSC profile of H48Q SOD1 contained three main endotherms (Fig. 7). Although T_{m1} was centered near 60°C for both WT and H48Q SOD1, the H48Q species began to unfold $\sim 5^\circ\text{C}$ below that of WT SOD1 and produced a broader endothermic transition. This indicated that this H48Q species was destabilized and suggested that it unfolded with less cooperativity compared with the WT species. The other two endotherms for H48Q, which most likely arose from unfolding of proteins containing bound metal ions, could not be definitively assigned to corresponding transitions of the WT enzyme.

DISCUSSION

We measured the thermal unfolding behavior of partially metallated species of WT and 14 mutant SOD1s associated with familial ALS (Table I). Copper and zinc ions were more likely to be bound to their correct sites in these biologically metallated proteins compared with SOD1 proteins remetalated *in vitro* (18, 24). Our initial experiments using DSC correlated increased metal contents with the unfolding of more stable SOD1 species (Fig. 2). For the WT and A4V mutants, we also identified the unfolding of copper-containing species at T_{m3} , whereas transitions at T_{m1} and T_{m2} most likely resulted from melting of SOD1 subunits lacking copper (Fig. 3).

Eight of the FALS-associated mutants (A4V, L38V, G41S, G72S, D76Y, D90A, G93A, and E133 Δ) shared copper coordination and specific activities comparable with WT SOD1 (18). For these “WT-like” mutants, T_{m2} was consistently $14\text{--}16^\circ\text{C}$ higher than T_{m1} , while T_{m3} was consistently $21\text{--}24^\circ\text{C}$ higher than T_{m1} (Table I). These results indicate that each mutant in this group preserved the structural interactions important for metal-induced stabilization. However, these WT-like mutants all exhibited reduced thermal stabilities when compared with corresponding WT SOD1 species (Table I).

Heating of four mutant SOD1s (G93A, G41S, G72S, and D76Y) produced an additional endotherm near 90°C (T_{m4}). The

appearance of this transition correlated with the mutant proteins containing the highest amounts of copper (Table I). Fully metallated bovine SOD1 unfolds at a similar temperature ($\sim 92^\circ\text{C}$) when heated at a comparable rate and concentration (5). We hypothesize that the transition at T_{m4} in our study arose from a subpopulation of SOD1s containing two Cu(II) and two Zn(II) ions per dimer, whereas T_{m3} reflected the unfolding of partially metallated species that contained copper.

A previous DSC analysis by Lepock *et al.* (22) of recombinant WT human SOD1 expressed in yeast produced major endotherms at 74.9°C (component 1) and 83.6°C (component 2). These transitions were assumed to arise from fully metallated species of SOD1 containing oxidized and reduced copper, respectively, but the total metal contents and the oxidation states of copper were not reported. Our results are consistent with those of Lepock *et al.* (22) if components 1 and 2 in their study correspond to the transitions at T_{m2} (species lacking copper but probably stabilized by zinc) and T_{m3} (partially metallated species containing copper) observed for WT SOD1 in the present work. This conclusion is also supported by the finding that human SOD1 proteins expressed in yeast may be undermetallated (19).

The T_m of a SOD1 subunit within a dimeric species probably depends on both its metal occupancy and its interactions with the partner subunit. In addition, the heating procedure during DSC may favor the rearrangement or consolidation of SOD1 species into more stable dimers (25). For example, denaturation or dissociation of a less stable subunit in a partially metallated dimer during slow heating would be expected also to decrease the stability of the partner subunit upon loss of strong intersubunit hydrophobic interactions. If monomerization of the partner occurs during heating, exposure of its hydrophobic dimer interface to the solvent would be thermodynamically unfavorable. The partner subunit may retain its full stability by reassociation with a similarly stable subunit to produce a new population of more completely metallated dimers.

Why did we observe a maximum of four distinct unfolding transitions for the biologically metallated SOD1 enzymes? If metal ions are incorporated into their proper sites, such that four potential metallation states exist for each SOD1 subunit (E-E, Cu-E, E-Zn, or Cu-Zn, where “E” refers to an empty metal binding site), then a total of 10 distinctly metallated dimeric SOD1 species or four monomeric species could be present in our samples. It is possible that many of these species exist but that the melting transitions within specific subsets overlap sufficiently to become indistinguishable by DSC. Alternatively, only a fraction of these possible species may occur *in vivo*, since metal ion incorporation into SOD1 may be a cooperative process (5). Prior stabilization by zinc binding, for example, might be important for biological incorporation of copper into SOD1.

Many of the mechanisms that have been proposed to explain FALS mutant SOD1 toxicity (14) presume an altered conformation of mutant compared with WT SOD1. Decreased mutant SOD1 stability may help to explain how >90 mutations scattered over more than one-third of the residues in this enzyme all cause a similar phenotype. The extreme thermochemical stability of fully metallated normal SOD1 implies that selection has occurred against less stable forms of the enzyme.

We have shown here that some FALS-associated SOD1 mutants are less stable than corresponding WT forms despite binding similar amounts of metal ions. We hypothesize that the observed thermal destabilization of the mutant enzymes *in vitro* may parallel a susceptibility to specific biochemical denaturing stresses *in vivo*. Although mutants such as D90A or G93A exhibited only a mild reduction in global stability as measured by DSC, it is possible that a more localized instabil-

ity may be pertinent to mutant SOD1 toxicity. Consistent with this view, D90A SOD1 exhibits an accelerated loss of dismutase activity compared with WT SOD1 upon exposure to either high temperature (73 °C, 3-fold acceleration) or denaturant (3.5 M guanidinium chloride, 6-fold acceleration) (26). While loss of dismutase activity itself is unlikely to be the toxic property of D90A SOD1, it may reflect a more ominous tendency of the enzyme to unfold locally.

For other SOD1 mutants, a decreased metal content greatly increases the fraction of destabilized protein. Six of the mutant proteins investigated here had substitutions that either perturb a copper ligand (H46R and H48Q) or may disrupt other important motifs in the metal binding region (G85R, D124V, D125H, and S134N). It is possible that metal loss from mutant SOD1 in the presence of other cellular denaturing influences may contribute to an increased burden of misfolded proteins at physiological temperatures. Indeed, recent analyses of SOD1 transgenic mice (27) or rats (28) indicate that those models expressing the metal-binding region mutants (H46R or G85R) exhibit frequent inclusion bodies recognized by antibodies to SOD1 or ubiquitin, while those models expressing the β -barrel pole mutants (G37R or G93A) exhibit fewer inclusions but more prominent vacuolar changes.

Our investigations of thermal stability for a large group of SOD1 variants associated with familial ALS have led to three significant observations: 1) distinct species within heterogeneous mixtures of partially metallated SOD1 can be effectively compared using DSC; 2) many mutants retain the ability to be stabilized upon metal ion binding or to be destabilized upon metal loss; and 3) all of the mutant proteins exhibit some degree of reduced stability compared with WT SOD1. The contribution of decreased SOD1 conformational stability to the pathogenesis of familial ALS remains to be explored in greater cellular and molecular detail.

REFERENCES

- McCord, J. M., and Fridovich, I. (1969) *J. Biol. Chem.* **244**, 6049–6055
- Bertini, I., Mangani, S., and Viezzoli, M. S. (1998) *Adv. Inorg. Chem.* **45**, 127–250
- Forman, H. J., and Fridovich, I. (1973) *J. Biol. Chem.* **248**, 2645–2649
- Lepock, J. R., Arnold, L. D., Torrie, B. H., Andrews, B., and Kruuv, J. (1985) *Arch. Biochem. Biophys.* **241**, 243–251
- Roe, J. A., Butler, A., Scholler, D. M., Valentine, J. S., Marky, L., and Breslau, K. J. (1988) *Biochemistry* **27**, 950–958
- Battistoni, A., Folcarelli, S., Cervoni, L., Polizio, F., Desideri, A., Giartosio, A., and Rotilio, G. (1998) *J. Biol. Chem.* **273**, 5655–5661
- Malinowski, D. P., and Fridovich, I. (1979) *Biochemistry* **18**, 5055–5060
- Mach, H., Dong, Z., Middaugh, C. R., and Lewis, R. V. (1991) *Arch. Biochem. Biophys.* **287**, 41–47
- Mei, G., Rosato, N., Silva, N., Jr., Rusch, R., Gratton, E., Savini, I., and Finazzi-Agro, A. (1992) *Biochemistry* **31**, 7224–7230
- Richardson, J., Thomas, K. A., Rubin, B. H., and Richardson, D. C. (1975) *Proc. Natl. Acad. Sci. U. S. A.* **72**, 1349–1353
- Tainer, J. A., Getzoff, E. D., Beem, K. M., Richardson, J. S., and Richardson, D. C. (1982) *J. Mol. Biol.* **160**, 181–217
- Tainer, J. A., Getzoff, E. D., Richardson, J. S., and Richardson, D. C. (1983) *Nature* **306**, 284–287
- Deng, H. X., Hentati, A., Tainer, J. A., Zafar, I., Cayabyab, A., Hung, W. Y., Getzoff, E. D., Hu, P., Herzfeld, B., Roos, R. P., Warner, C., Deng, G., Soriano, E., Smyth, C., Parge, H. E., Ahmed, A., Roses, A. D., Hallewell, R. A., Pericak-Vance, M. A., and Siddique, T. (1993) *Science* **261**, 1047–1051
- Cleveland, D. W., and Rothstein, J. D. (2001) *Nat. Rev. Neurosci.* **2**, 806–819
- Hart, P. J., Liu, H., Pellegrini, M., Nersissian, A. M., Gralla, E. B., Valentine, J. S., and Eisenberg, D. (1998) *Protein Sci.* **7**, 545–555
- Borchelt, D. R., Lee, M. K., Slunt, H. S., Guarnieri, M., Xu, Z. S., Wong, P. C., Brown, R. H., Jr., Price, D. L., Sisodia, S. S., and Cleveland, D. W. (1994) *Proc. Natl. Acad. Sci. U. S. A.* **91**, 8292–8296
- Ratovitski, T., Corson, L. B., Strain, J., Wong, P., Cleveland, D. W., Culotta, V. C., and Borchelt, D. R. (1999) *Hum. Mol. Genet.* **8**, 1451–1460
- Hayward, L. J., Rodriguez, J. A., Kim, J. W., Tiwari, A., Goto, J. J., Cabelli, D. E., Valentine, J. S., and Brown, R. H., Jr. (2002) *J. Biol. Chem.* **277**, 15923–15931
- Goto, J. J., Gralla, E. B., Valentine, J. S., and Cabelli, D. E. (1998) *J. Biol. Chem.* **273**, 30104–30109
- Pace, C. N., Vajdos, F., Fee, L., Grimsley, G., and Gray, T. (1995) *Protein Sci.* **4**, 2411–2423
- Edge, V., Allewell, N. M., and Sturtevant, J. M. (1985) *Biochemistry* **24**, 5899–5906
- Lepock, J. R., Frey, H. E., and Hallewell, R. A. (1990) *J. Biol. Chem.* **265**, 21612–21618
- Liu, H., Zhu, H., Eggers, D. K., Nersissian, A. M., Faull, K. F., Goto, J. J., Ai, J., Sanders-Loehr, J., Gralla, E. B., and Valentine, J. S. (2000) *Biochemistry* **39**, 8125–8132
- Goto, J. J., Zhu, H., Sanchez, R. J., Nersissian, A., Gralla, E. B., Valentine, J. S., and Cabelli, D. E. (2000) *J. Biol. Chem.* **275**, 1007–1014
- Brandts, J. F., and Lin, L. N. (1990) *Biochemistry* **29**, 6927–6940
- Marklund, S. L., Andersen, P. M., Forsgren, L., Nilsson, P., Ohlsson, P. I., Wikander, G., and Oberg, A. (1997) *J. Neurochem.* **69**, 675–681
- Watanabe, M., Dykes-Hoberg, M., Cizewski Culotta, V., Price, D. L., Wong, P. C., and Rothstein, J. D. (2001) *Neurobiol. Dis.* **8**, 933–941
- Nagai, M., Aoki, M., Miyoshi, I., Kato, M., Pasinelli, P., Kasai, N., Brown, R. H., Jr., and Itoyama, Y. (2001) *J. Neurosci.* **21**, 9246–9254
- Hosler, B. A., Nicholson, G. A., Sapp, P. C., Chin, W., Orrell, R. W., de Bellerocche, J. S., Esteban, J., Hayward, L. J., McKenna-Yasek, D., Yeung, L., Cherryson, A. K., Dench, J. E., Wilton, S. D., Laing, N. G., Horvitz, R. H., and Brown, R. H., Jr. (1996) *Neuromusc. Disord.* **6**, 361–366